Reconstruction of intrinsic parameters of a composite from the measured frequency dependence of permeability

2002 J. Phys.: Condens. Matter 14 9507

(http://iopscience.iop.org/0953-8984/14/41/308)

INSTITUTE OF PHYSICS PUBLISHING JOURNAL OF PHYSICS: CONDENSED MATTER

J. Phys.: Condens. Matter **14** (2002) 9507–9523 PII: S0953-8984(02)38144-X

Reconstruction of intrinsic parameters of a composite from the measured frequency dependence of permeability

A V Osipov, K N Rozanov, N A Simonov and S N Starostenko

Institute for Theoretical and Applied Electromagnetics, 13/19 Izhorskaya ul., 125412 Moscow, Russia

E-mail: k_rozanov@mail.ru

Received 13 July 2002, in final form 30 August 2002
Published 4 October 2002
Online at stacks.iop.org/JPhysCM/14/9507

Abstract

The mixing rules for the permittivity and permeability of composites are known to depend greatly on the microscopic structure of the composite. This dependence can be quantified in terms of Bergman's spectral function. In this paper, the spectral function of actual magnetic composites is reconstructed from their measured microwave constitutive parameters.

The samples under study are composed of carbonyl iron or Fe–Cr–Al alloy powders embedded in a paraffin wax matrix. The permittivity and permeability of the samples is measured in the 0.1–10 GHz frequency band. The proposed approach to process the measured data allows the spectral function of the composite and frequency dependence of intrinsic permeability of inclusions to be derived. The obtained results are in agreement with available tabulated data.

1. Introduction

The key problem in the physics of composites is how to determine their average, or effective properties [1]. For this purpose, a number of approximate equations, usually referred to as the mixing rules, are known. The mixing rules allow the susceptibilities of a mixture to be predicted based on the data of the individual properties and the volume fraction of the constituents and these rules have the same form for all transport properties such as thermal or electrical conductivity, diffusion coefficient etc [2, 3]. This paper deals with the microwave constitutive parameters, the permittivity ε and the permeability μ, of an asymmetrical mixture, where discrete inclusions are embedded in a matrix with different properties. The mixing rules conventionally used for such cases include the Maxwell dilute limit formula [4], the

Maxwell Garnett mixing rule [5], Bruggeman's effective medium approximation (EMA) [6], the differential EMA (see, e.g., [7]), McLachlan's generalized effective medium theory [8] etc. Extensive lists of known mixing rules are given, e.g., in [8, 9].

The reliability of a mixing rule is conventionally determined by examining the static permittivity or permeability as a function of the volume fraction of inclusions. However, the effective parameters of actual composites are dependent not only on the concentration of inclusions but also on their distribution, i.e., on the microstructure of the composite. Because of this, for example, composites containing conducting inclusions of spherical shape may exhibit the percolation transition at volume concentrations anywhere between 5 and 50% [10], depending on the particle size distribution, mixing technology and physico-chemical properties of the inclusions and matrix. Due to various microstructures, the effective constitutive parameters of a composite at a certain volume fraction of inclusions can have values within a rather wide range bounded by the Wiener limits [11]. Every known mixture rule corresponds to a particular microstructure of the composite and therefore describes adequately only that particular mixture.

Another approach to check the validity of mixing rules involves the examination of the frequency dependence of the permittivity and/or permeability of a composite. The advantage is that a sample of fixed concentration is under study and, therefore, possible variations of the microstructure with concentration need not be considered, unlike the case of examining the concentration dependence.

This approach is not universal. Its application is possible if

(a) the frequency dispersion of the constitutive parameters of both the inclusions and the matrix is known and
(b) a pronounced frequency dispersion of the constitutive parameters of the composite occurs within the measured frequency range.

When the permittivity of a metal–dielectric mixture is the property under consideration, the first of these requirements is typically met. Most dielectrics and metals are characterized by the frequency independent permittivity or conductivity, respectively, at least up to the far IR range. But the location of the dispersive region depends strongly on the shape and conductivity of the inclusions [12]. Hence the experimental observation of the frequency dispersion of the permittivity is not an easy task in many occasions.

The situation is the opposite in the case of microwave effective permeability. The intrinsic permeability of most magnetics is greatly dispersive at microwaves due to the ferromagnetic resonance and the domain walls motion. In addition, eddy currents affect the intrinsic permeability of conducting particles. Because of this, magnetic composites exhibit a variety of types of microwave frequency dispersion, which can be exploited to validate the mixing rules.

On the other hand, the intrinsic permeability is not determined solely by the composition of the inclusions and depends strongly on the structure and the method of production of these inclusions. That is why the magnetic properties of thin powders and bulk material of the same composition vary greatly for many materials, and the permeability values of magnetic inclusions in composites should not be taken for granted.

It might seem that studying the constitutive parameters of diluted composites can readily solve this problem. The cooperative effects are negligible in these, and the permeability of inclusions can be extracted from the experimental data on the effective permeability using the dilute limit mixing rule. After that, the frequency dependence of permeability obtained can be used to calculate the effective permeability at high concentrations of the inclusions. However, in many practical occasions the effect of composite microstructure is essential

even in dilute mixtures. This is evidenced, for example, by the experimental data on the composites consisting of paraffin wax matrix and carbonyl iron powder [13]. The shape of carbonyl iron particles is well known to be almost spherical. In the dilute limit, the effective permittivity is a linear function of the concentration p, $\varepsilon_e/\varepsilon_h = 1 + p/k$, where ε_h is the host permittivity and $k = 1/3$ for spherical inclusions. The measured dependence [13] is linear as well but the fitted value of k is 0.15. The same result of $k = 0.13$–0.18 has been obtained for composites filled with carbonyl iron in the present study, see section 3 for details. The breakdown of the dilute limit can only be explained by the formation of aggregates of iron particles, which dramatically enhance the effective permittivity. This might be the reason why archived data on the microwave intrinsic permeability of ferromagnetic metal powders are rarely available.

Thus the microstructure is essential in analysing the experimental data on the constitutive parameters. The relation between the constitutive parameters of a composite and its microstructure involves the correlation functions of all orders for the spatial distribution of inclusions in the matrix [14], which is hard to find from the experiment. There is an alternative approach to account for the microstructure that is provided by the theory developed by Bergman and Milton [2, 3, 14–19]. The theory treats the general analytical properties of constitutive parameters of a mixture. A universal characteristic of the microstructure is the spectral function that represents a normalized constitutive parameter of the mixture as a function of that of the components. The same spectral function governs all transport properties including both permittivity and permeability and depends only on the microgeometry, i.e., on the shape of the inclusions and their spread in size and location. The theory is valid for all concentrations, including those above the percolation threshold.

It is problem of great interest to determine the spectral function of actual composites. This function can be used for the analysis of the microscopic structure of the composites or for the correction of mixing rules. However, as is shown below, this problem is hard to solve. That is why experimental attempts to obtain the spectral function of actual composites from measured data are rare [20, 21]. In these papers, the IR frequency dependence of the reflectance was exploited for reconstructing the spectral function. The concept of spectral function was also used to improve the mixing rule describing the experimental conductivity of porous rocks saturated with a conducting brine [18].

In the present paper, the Bergman–Milton theory is used to reconstruct the spectral function of actual magnetic composites and the intrinsic permeability of magnetic metal inclusions based on the experimental data on microwave constitutive parameters of the composite. The composites under study are two-component mixtures consisting of paraffin wax and metal powders, namely carbonyl iron or Fe–Cr–Al alloy. The volume fraction of powders is in the range of 1–55%. The permittivity and permeability are measured with the use of short circuit and open circuit coaxial cells. The details of the measurement technique and experimental data will be published elsewhere. The aim of this paper is to reveal the possibility of obtaining the frequency dependence of microwave permeability of magnetic powders and the spectral function of composites from the measured effective constitutive parameters.

The paper is organized as follows. The first section summarizes the general properties of the spectral function, which are essential in further discussion. In particular, these properties are considered more closely for the case of a characteristic spectral function with a continuous pole distribution, which is the most closely related to the properties of actual composites. The second section describes the model used to extract the frequency dependence of the permeability of inclusions and the spectral function of the composite from the experimental data. In the third section, the results obtained are presented and discussed. In the conclusion, possible ways to refine the obtained data are sketched.

2. The Bergman–Milton theory of composites

This section contains a summary of the Bergman–Milton theory of composites [14–19]. In this theory, the same formalism is applied to the description of all transport parameters of the composite. In this section, for the sake of definiteness, the permittivity of composites is treated.

The basic concept of the Bergman–Milton theory is the characteristic geometrical function, which is usually referred to as the spectral function in recent literature. In the case of a two-component composite the spectral function relates the permittivity of a mixture to the ratio of the permittivity of inclusions to that of the matrix. This function depends only on the microstructure of the composite [15]. It can be defined in several alternative ways, the most conventional definition,

$$F(s) = 1 - \frac{\varepsilon_e}{\varepsilon_h}, \qquad s = \frac{1}{1 - \varepsilon_i/\varepsilon_h} \tag{1}$$

being used in this paper. In equation (1), the subscripts e, i and h relate respectively to the effective medium (mixture), inclusions and host (matrix). For perfectly conducting inclusions, $s = 0$.

In the static case, s is located at the real axis. When the frequency dependence is under treatment, the spectral function must be regarded as a function of the complex argument. It has simple analytical properties [15]. If inclusions are of ellipsoidal shape, the spectral function of a composite sample of a finite size has a finite number of poles. All the poles are located between zero and unity, the residues of these being real positive quantities less than unity. Therefore, the spectral function can be written as a series:

$$F(s) = \sum_{n=0}^{N} \frac{B_n}{s - s_n}, \qquad 0 < B_n < 1,\ 0 \leqslant s_n < 1. \tag{2}$$

The interval $0 \leqslant s < 1$, where all the poles are located, corresponds to the negative values of the permittivity of inclusions ε_i provided that ε_h is positive. The exact locations and residues of the poles depend on the microstructure of the sample. The only limitation on these values is due to the following two sum rules [15], that hold for any volume fraction of inclusions p:

$$\sum_{n=0}^{N} B_n = p, \qquad \sum_{n=0}^{N} s_n B_n = \frac{p(1-p)}{D}. \tag{3}$$

In (3), D is the dimensionality of the sample, being equal to two for planar structures and three for bulk composites. The first of equations (3) is valid for any composite; the second one governs isotropic mixtures only.

Following the paper [16], the relation between the pole pattern of the spectral function and the microstructure of the composite is considered more closely here. A simple example of a composite is a diluted mixture of non-interacting ellipsoidal inclusions with identical shape and orientation. This case is described by the Maxwell dilute limit mixing rule, that can be transformed to the spectral function as

$$F(s) = \frac{p}{s - L}, \tag{4}$$

where L is the depolarization factor of the inclusions along the external field. The spectral function (4) has a single pole at $s = L$, with the residue equal to the concentration of the inclusions, $B_0 = p$.

With this in mind, the series representation (2) of the spectral function can be interpreted as the mixing rule for a hypothetical system of non-interacting ellipsoidal inclusions, with

depolarization factors L_n and the volume fractions B_n. Note that the poles of spectral function are actually related not only to the shape of inclusions but also to the interaction between inclusions.

Another example of the spectral function having a single pole is provided by the Maxwell Garnett mixing rule that is valid for any concentration of identical, spherically shaped and equally spaced inclusions in a composite. It is the Maxwell Garnet mixing rule that follows from the assumptions that the spectral function of an isotropic three-dimensional ($D = 3$) medium has a single pole. The related spectral function is readily produced by the solution of (3) as

$$F(s) = \frac{p}{s - (1-p)/3}. \tag{5}$$

The comparison of (4) and (5) shows that the additional factor $(1 - p)$ appears in the latter equation. This factor accounts for the dipole interaction between inclusions. The pole $s_0 = (1 - p)/3$ relates to the famous Lorentz dielectric catastrophe [4], where both the local electric fields and the effective permittivity tend to infinity. All modifications of the Maxwell Garnett mixing formula, such as the Odelevski formula [22], correspond to a single-pole approximation of the spectral function.

The origin of multiple poles in the spectral function is examined in [15]. These are shown to be related to either the variety of shapes of inclusions or strong interaction between neighbouring inclusions, when higher order modes of the electric field are excited. If the interaction is weak, then only the eigenmode is excited. If, in addition, the inclusions are ellipsoidal in shape and indistinguishable, then the spectral function has a single pole as in (4), (5). If the interaction is weak but the inclusions are differently shaped or oriented, then the distribution of poles represents the spread in the shape of inclusions along the external field. In non-ellipsoidal inclusions, a multitude of poles also appears. The pole distribution in the spectral function is the most complicated when the concentration of inclusions is so high that a clustered structure appears. Then the total number of poles is approximately the product of the number of excited modes and the number of inclusions. The percolation threshold corresponds to the spectral function with the least pole location equal to zero [15], as the permittivity of a mixture filled with metal inclusions tends to infinity at the threshold.

It is of interest to regard the EMA mixing rule in terms of the Bergman–Milton theory. It might seem that Bruggeman's formula [6] contradicts the theory since its spectral function is given by

$$F^{EMA}(s) \equiv 1 - \frac{\varepsilon_e^{EMA}}{\varepsilon_h} = 1 - \frac{1}{4}\left((1-3p)\frac{1}{s} + 1 \mp \sqrt{\left((1-3p)\frac{1}{s}+1\right)^2 + 8\left(1 - \frac{1}{s}\right)}\right). \tag{6}$$

Equation (6) produces no poles at any concentration of inclusions below the percolation threshold, $p = 1/3$. However, the EMA mixing rule is shown [15] to correspond to the spectral function having a continuous distribution of poles with the singularities merging in a branch cut. The branch cut is located within the [0,1) range of the argument s, and the left branch point is zero at the percolation threshold in agreement with the Bergman theory.

As mentioned above, in actual composites a multitude of poles can be observed as a rule. In this case, the analysis can be simplified by substituting the exact discrete distribution of poles by a continuous distribution corresponding to a branch cut at the complex plane of s, similarly to the spectral function of EMA [6]. The properties of the spectral function with the continuous distribution of poles [14, 18] are analogous to those of the discrete spectral

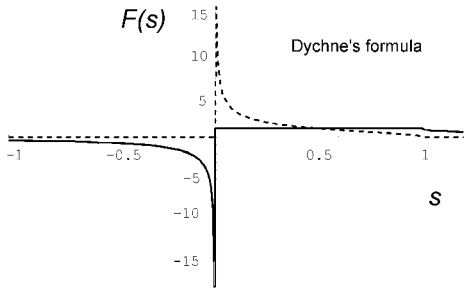

Figure 1. The spectral function for Dykhne's equation [20]. The solid curve shows the real part; the dashed curve shows the imaginary part.

function. For the continuous case, (2) transforms to

$$F(s) = \int_0^1 \frac{B(x)}{s - x}\,\mathrm{d}x, \qquad B(x) \geqslant 0. \tag{7}$$

Since the integral in (7) is defined for the values of s located beyond the branch cut only, it is reasonable to define $F(s)$ at the branch cut as $F(s - \mathrm{i}0)$.

Similarly, sum rules (3) transform to

$$\int_0^1 B(x)\,\mathrm{d}x = p, \qquad \int_0^1 xB(x)\,\mathrm{d}x = \frac{p(1-p)}{D}. \tag{8}$$

As in the discrete case, the first equation in (8) holds for any composite and the second one is valid for an isotropic mixture only. The physical meaning of the spectral function with the continuous pole distribution differs from that of the case when the distribution is discrete [15]. Namely, the function $F(s)$ given by (7) is representative of a set of composites, which are macroscopically identical but different in the microgeometry. Therefore, $B(x)$ in (7) relates to the weighted density of poles within the range $(x, x + \mathrm{d}x)$.

A feature of spectral functions with the continuous pole distribution is that the imaginary part of these is proportional to the density of the pole distribution,

$$\mathrm{Im}\, F(s - \mathrm{i}0) = \pi B(s). \tag{9}$$

To illustrate the features of the spectral function with the continuous pole distribution, we calculate the spectral function for two examples of heterogeneous medium models, the EMA model and Dykhne's theory [23]. Dykhne's equation provides an exact description of a two-dimensional isotropic structure at the percolation threshold, $p = 1/2$, and is written as $\varepsilon_e = \sqrt{\varepsilon_i \varepsilon_h}$, which readily transforms to the spectral function given by

$$F(s) \equiv 1 - \frac{\varepsilon_e}{\varepsilon_h} = 1 - \sqrt{\frac{s-1}{s}}. \tag{10}$$

This function is plotted in figure 1. The branch cut of function (10) is located within the interval [0,1), the left branching point being equal to zero in agreement with the Bergman theory. The density of the pole distribution $B(x)$ readily follows from (9) and (10) as

$$B(x) = \frac{1}{\pi}\sqrt{\frac{1-x}{x}}. \tag{11}$$

The integration of $B(s)$ reveals that both sum rules (8) hold at $p = 1/2$ and $D = 2$.

In figure 2, the calculated EMA spectral functions (6) are given, with the concentration of inclusions $p = 0.002$, 0.02, 0.1 and 0.2. The solid and dashed curves show the real

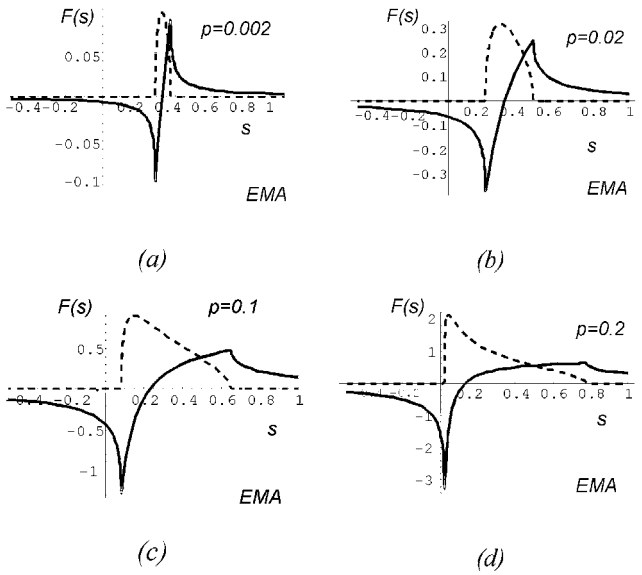

Figure 2. The spectral functions for the EMA model. The concentration of inclusions p is (a) $p = 0.002$, (b) $p = 0.02$, (c) $p = 0.1$ and (d) $p = 0.2$. The solid curve shows the real part; the dashed curve shows the imaginary part.

and imaginary parts of $F(s)$, respectively. According to (9), the imaginary part of $F(s)$ is proportional to the density of the pole distribution $B(x)$. It is seen from the figure that the EMA spectral function looks like the single-pole spectral function (4) only at very low p. The spread in the pole density distribution, which is evidence for the cluster formation, is clearly seen at as low a concentration as $p = 0.02$. With p tending to the percolation threshold, the left branching point tends to zero and the right branching point tends to unity. The numerical study reveals that that sum rules (8) hold at $p < 1/3$. At $p > 1/3$, the width of the branch cut decreases with the concentration but an additional isolated pole at $s = 0$ appears. If this pole is taken into account, the sum rules hold as well.

3. The approach to extract the intrinsic properties from the measured data

The purpose of this paper is to show the possibility of obtaining the frequency dependence of microwave permeability of magnetic powders and the spectral function of composites from the measured effective constitutive parameters. The solution for the problem implies that two functional dependences, the permeability as a function of frequency and the spectral function as a function of normalized permeability of inclusions, should be found from a single one, the frequency dependence of the effective permeability of the composite.

Thus the formulated problem is obviously ill defined and a definite solution can be found only in some particular cases. For example, suppose that the pole distribution in the spectral function is very narrow, as it is in the Maxwell Garnett mixing rule. As seen from the above consideration, the frequency dependence of the intrinsic permeability is readily reconstructed from the measured effective permeability. However, this analysis produces no data on the details of the pole density function.

The opposite case occurs when the intrinsic permeability exhibits a high quality factor resonance. This occasion is illustrated by figure 3, where the calculated frequency dependence

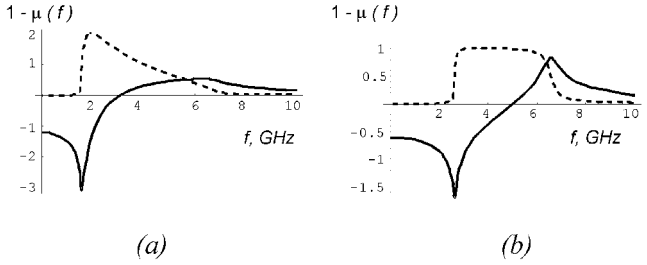

Figure 3. The frequency dependence of permeability for two hypothetical mixtures with concentrations of inclusions $p = 0.2$: (a) the EMA, for the spectral function see figure 2(d); (b) the model of trapezium-like form of the pole distribution with $s_0 = 0.1$, $s_1 = 0.7$, $a = 0.5$, for the spectral function see figure 4(c). The intrinsic permeability of inclusions is given by (14) with $f_0 = 1$ GHz, $S = 60$ GHz and $\alpha = 0.01$. The solid curve shows the real part; the dashed curve shows the imaginary part.

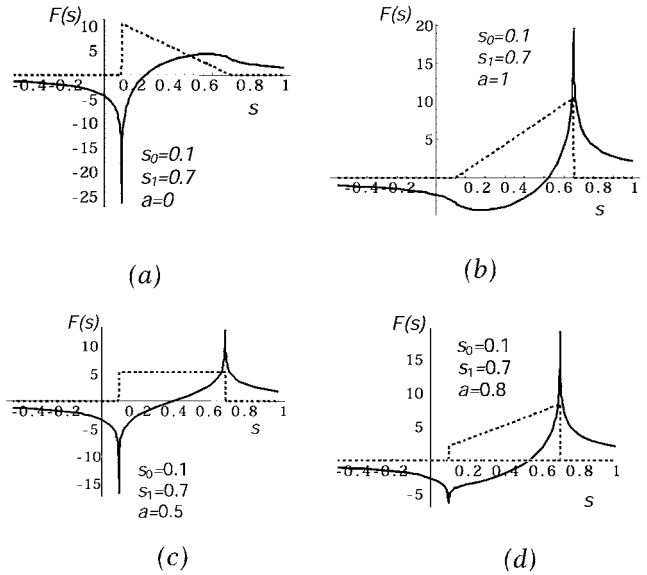

Figure 4. The linear-piecewise trapezium-like spectral function with the continuous pole distribution, see (12), (13), at $s_0 = 0.1$, $s_1 = 0.7$ and different values of a: (a) $a = 0$, (b) $a = 1$, (c) $a = 0.5$ and (d) $a = 0.8$. The solid curve shows the real part; the dashed curve shows the imaginary part.

of permeability is presented for two hypothetical mixtures having the same volume fraction, $p = 0.2$, but different spectral functions, namely, the EMA spectral function and a rectangle-like pole distribution function, which is defined by (12), (13) and shown in figure 4(c). In both the cases, the intrinsic permeability is assumed to be governed by the Landau–Lifshitz equation, see (14), with $f_0 = 1$ GHz, $S = 60$ GHz and $\alpha = 0.01$. The comparison of the spectral functions shown in figures 2(a) and 4(c) with the dependences given in figure 3 reveals that the form of the frequency dependences of the effective permeability is very close to the related spectral function.

The reason is that for a high quality resonance of the permeability the argument of the spectral function, $s = 1/(1 - \mu(f))$, depends linearly on f and at frequencies above

the resonance possesses a negative real part and negligible imaginary part. Hence at these frequencies s is located in the close vicinity of poles of $F(s)$ and the frequency dependence of the permeability replicates the shape of the spectral function. Then the latter can be extracted with high accuracy from the measured effective permeability. But no refinement of the data on the intrinsic permeability near resonance can be obtained in this case, of course.

To make the problem more definite, additional data on the intrinsic properties of the composite must be introduced. For this purpose, both the data on permeability and permittivity of the composite are processed simultaneously in this study. This provides some additional data, as the effective permittivity and permeability are governed by the same spectral function. However, the microwave permittivity of conducting inclusions is very high, and only the value of the spectral function at $s = 0$ can be extracted from the effective permittivity of the composite. In addition, the experimental data processing involves simultaneous treatment of data on composites with different volume fractions of the same inclusions. For these data, the intrinsic permeability is the same, which allows the uncertainty in the results to be diminished.

To obtain further reduction of the uncertainty, a simplified model of the intrinsic properties of composites is accepted. Both the frequency dependence the of permeability and the spectral function were approximated by some probe functions, which depend on a few real parameters that must be varied to obtain the best fit of the experimental data. This reduces the problem of two unknown functional dependences to a finite number of unknown parameters, which provide a reasonable fit of these functions. Note that the use of known mixing rules to obtain the probe function for $F(s)$ is not a good idea, as most of these allow no variations in the form of spectral function, which may be quite different from that of actual composites.

We use the probe function for $F(s)$ that corresponds to a linear-piecewise trapezium-like form of $B(x)$ represented by a sum of two triangle-like functions with the same base but opposite slopes, see figure 4. This allows us to define a wide range of branching point locations and of shapes of pole density distribution by varying as few as three parameters. The related spectral function is obtained by substituting the trapezium-like function $B(x)$ into (7) and by accounting for the first equation (8), that yields

$$F(s) = (aG(s, s_0, s_1) + (1 - a)G(s, s_1, s_0))\,p, \tag{12}$$

where s_0, s_1 are the left and right branching points, a is the weight factor determining the form of the function $B(s)$, p is the volume fraction of inclusions and G is given by

$$G(s, s_k, s_l) = 2\frac{s_k - s_l + (s_k - s)\ln\left(\frac{s-s_k}{s-s_l}\right)}{(s_k - s_l)^2}. \tag{13}$$

In (13), the logarithm is regarded as a complex function. The values of s_0, s_1 and a are limited by inequalities $0 \leqslant s_0 \leqslant s_1 < 1$, $0 \leqslant a \leqslant 1$. Notice that if s is within the interval (s_0, s_1), then $(s - s_0)/(s - s_1) < 0$ and the function (11) has an imaginary part, see figure 4.

The probe function for the frequency dependence of the intrinsic permeability is based on the Landau–Lifshitz equation. If the particles are of spherical shape and Snoek's law is taken into account, then this equation leads to the frequency dependence of the susceptibility given by [24, 25]

$$\chi_0(f, f_0, \alpha) = \frac{1}{4\pi}\frac{S}{f_0}\frac{1 + \mathrm{i}\alpha f/f_0 + \alpha^2}{1 - (f/f_0 - \mathrm{i}\alpha)^2}, \tag{14}$$

with Snoek's constant $S = \gamma 4\pi M_s$, the saturation magnetization $4\pi M_s$, the gyromagnetic ratio $\gamma = 2.8$ GHz kOe^{-1}, the resonance frequency f_0, the operating frequency f and the Gilbert damping factor α. For pure iron, $M_s = 1700$ G and hence $S \cong 60$ GHz. The additional averaging factor $2/3$ should be introduced for polycrystalline particles [24], giving $S \cong 40$ GHz.

As the ferromagnetic powders under study are highly permeable polycrystalline magnetics, strong coupling between the granules in the powder particles must occur. In this case the magnetic properties of inclusions are described by a continuous distribution of ferromagnetic resonance frequencies, each resonance relating to a resonant mode of the cluster as a whole rather than to a mode of an isolated crystallite [24]. For the sake of simplicity, a rectangular distribution function of the resonance is accepted in this study:

$$\mu_i(f) = 1 + \frac{4\pi}{F_1 - F_0} \int_{F_0}^{F_1} \chi_0(f, f_0, \alpha)\, \mathrm{d}f_0. \tag{15}$$

The values of damping factor α are assumed to be the same for all resonances.

As the powders under study are conducting, it is also necessary to take into account the effect of the eddy current on the intrinsic permeability. The composites with concentration well below the percolation threshold are involved in this study. Therefore, the collective skin effect is negligible. The skin effect at individual inclusions is accounted for by the renormalization of the intrinsic permeability of spherical inclusions using Lewin's formula [26]:

$$\begin{aligned} &\tilde{\mu}_i = \mu_i C(2\pi(1 - \mathrm{i})r/\delta), \\ &C(z) = 2\frac{\sin z - z\cos z}{(z^2 - 1)\sin z + z\cos z} \end{aligned} \tag{16}$$

where f is the frequency, GHz, r is the mean radius of inclusion and δ is the skin depth. To characterize the skin effect at the inclusions, it is convenient to introduce the value θ that is the ratio of the average radius of inclusions, r, to the skin depth of the non-magnetic conducting inclusion at 1 GHz.

Thus the model used in this study is dependent on the parameters S, F_0, F_1, α and θ determining the intrinsic permeability of the inclusions, and s_0, s_1 and a determining the spectral function of the composite. As the data on two concentrations of the inclusions are processed simultaneously, two different spectral functions are involved in each calculation with the result of a total of 11 independent parameters. These parameters are varied to obtain numerically the least mean squares fit of the experimental data on the measured low frequency permittivity and microwave permeability of the composites by the above model.

A standard minimization routine was used for this purpose. Note that in the mathematical meaning the problem described above is still not well conditioned. Because of this, and also due to the presence of measurement uncertainty, the square root difference as a function of the varied parameters has a wide minimum with a noticeable ripple. This leads to the uncertainty in the results of the minimization, which may be rather different when the routine starts from different initial points. This discrepancy can be used for determining the accuracy of the obtained values of intrinsic permeability and the spectral function. To do this, the fitting procedure is started 20 times from different starting points. Among the results of this procedure, only those of which the resulting relative square root difference does not exceed 15%, i.e., those satisfying the conventional goodness-of-fit test $\chi^2 \leqslant n$ [27], where n is the number of degrees of freedom, are retained. The average of these results produces the most probable values of the parameters, while the rms of these yields the accuracy.

4. Results and discussion

The composite samples consist of magnetic powders embedded into paraffin wax matrix. Two types of powder, carbonyl iron and 13.6 at.% Cr–6 at.% Al–80.4 at.% Fe alloy, are examined in this study. The mean size of the powder particles is about 6 μm for carbonyl iron and about

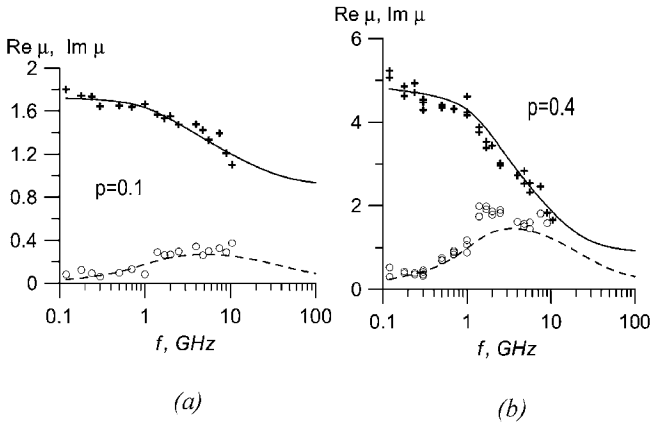

Figure 5. The measured microwave permeability of composites filled with carbonyl iron powder at two concentrations of inclusions p: (a) $p = 0.1$ and (b) $p = 0.4$. Crosses denote the real part and circles denote the imaginary part of measured permeability. The curves are the fit with the model used.

60 μm for the alloy. The volume fraction of the powder in composite samples is within 1–55%, the precise values being obtained by the measurement of density.

The microwave effective permittivity and permeability values of the samples are obtained in the 0.1–10 GHz frequency range from the measured complex reflection coefficient. At frequencies below 2.5 GHz, the measurement is made with open-circuit and short-circuit 50 Ω coaxial measuring units. Both the units are 3.04 mm in the diameter of the inner conductor, 7.00 mm in the diameter of the outer conductor and 50 mm in length. For higher frequencies, the measurement is made with the short-circuit unit alone, coaxial dielectric inserts of 5, 10 or 20 mm in height being placed onto its bottom. The relative measurement uncertainty in both permittivity and permeability varies from 5% in the 0.1–5 GHz range to 15% at 10 GHz. To eliminate the effect of gaps between the sample and the conductors on the measured parameters, the die-pressed samples are heated and pressed directly in the units. A typical result of the measurement and the result of data processing with the above model is shown in figure 5.

Figure 6 illustrates the importance of accounting for the microstructure of the composites under study. In the figure, the plot is shown of the measured volume fraction dependence of low frequency permittivity and permeability for the composites filled with carbonyl iron powder. The dependences are approximately linear, $\varepsilon_e/\varepsilon_h = 1 + p/k$ and $\mu_e = 1 + p/k$, at $p < 0.1$ with the slope $k = 0.18$ for both dependences. This value is less than half that predicted for spherical inclusions by the Maxwell dilute limit, $k = 1/3$. This is evidence of the fact that the clusters of iron inclusions affect the properties of the mixture even when the volume fraction of the inclusions is as low as 1%. Therefore, to describe these mixtures it is necessary to introduce the spectral function.

The processing of the measured data is made with the volume fraction of inclusions being 10 and 40% for carbonyl iron and 15 and 37% for Fe–Cr–Al-alloy. All these composites are below the percolation threshold. The values of the parameters introduced in the previous section and the standard deviation of these are given in tables 1–3.

It is seen from the tables that the mixtures of identical concentration with carbonyl iron and with Fe–Cr–Al alloy have quite different spectral functions. For example, for the composite filled with 37% of alloy, the lower branching point is 100 times less than that for the carbonyl iron at $p = 0.4$. To understand this difference, notice that the particles of carbonyl iron include

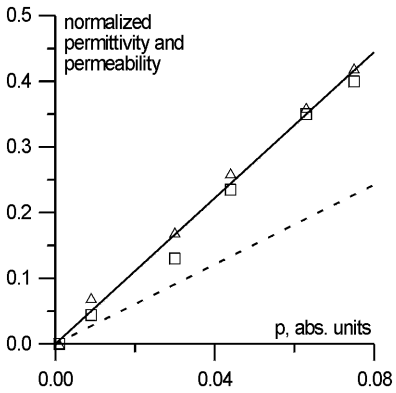

Figure 6. The measured volume fraction dependence of normalized low frequency permittivity, $\varepsilon_e/\varepsilon_h - 1$ (boxes), and permeability, $\mu_e - 1$ (triangles), for composites filled with carbonyl iron powder. The dashed line corresponds to the Maxwell dilute limit (4) for metal spherical inclusions ($L = 1/3$); the solid line corresponds to $L = 0.18$.

Table 1. The results for the intrinsic permeability and skin effect of materials under study.

Material	S (GHz)	F_0 (GHz)	F_1 (GHz)	α	θ
Carbonyl iron	57 ± 3	0	0.28 ± 0.2	2 ± 1	0.3 ± 0.2
Fe–Cr–Al alloy	33 ± 5	$(1.2 \pm 0.7) \times 10^{-5}$	$(5 \pm 4) \times 10^{-3}$	0.4 ± 0.2	1.6 ± 0.3

Table 2. Parameters of the spectral function for composites filled with carbonyl iron at different concentrations.

p	s_0	s_1	a
0.05	0.01 ± 0.003	0.5 ± 0.05	0.2 ± 0.1
0.10	0.015 ± 0.004	0.56 ± 0.06	0.4 ± 0.1
0.15	0.01 ± 0.003	0.55 ± 0.05	0.3 ± 0.1
0.40	0.01 ± 0.002	0.5 ± 0.05	0.15 ± 0.08

Table 3. Parameters of the spectral function for composites filled with Fe–Cr–Al alloy at different concentrations.

p	s_0	s_1	a
0.15	0.005 ± 0.001	0.6 ± 0.03	0.5 ± 0.07
0.37	$0.000\,25 \pm 0.000\,04$	0.7 ± 0.07	0.2 ± 0.1

a flocculent oxide shell of about 0.1 μm in thickness [28], while the oxide film at the surface of alloy particles is much thinner. Due to that, the least distance that is possible between metal cores of Fe–Cr–Al particles is much less than that of the carbonyl iron particles. Therefore, the composite filled with the alloy particles at $p = 0.37$ appears to be much closer to the percolation threshold than the composite filled with the carbonyl iron at $p = 0.4$.

Figures 7–10 show the data on the intrinsic permeability of the inclusions and the spectral functions for some of the composites under study. It is seen from the figures that although the uncertainty in the parameters of the model is rather large, the obtained frequency dependences of intrinsic permeability and the spectral function of composites seem to be definite enough. The spectral functions shown in figures 9 and 10 are determined with higher accuracy than the

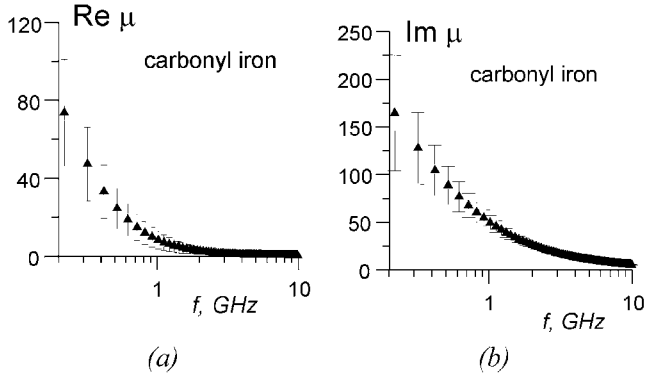

Figure 7. The average values (triangles) and the standard deviation of reconstructed intrinsic permeability of carbonyl iron.

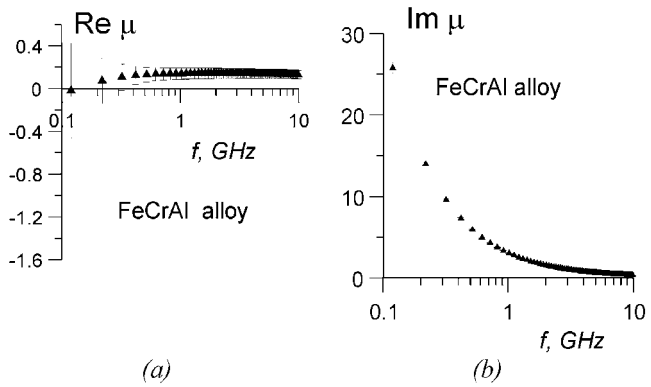

Figure 8. The average values (triangles) and the standard deviation of reconstructed intrinsic permeability of FeCrAl (13.6 at.% Cr–6 at.% Al–80.4 at.% Fe) alloy.

frequency dependences of intrinsic permeability shown in figures 7 and 8. The permeability dispersion curve of carbonyl iron, see figure 7, is of relaxation type. The curve obtained for the alloy (figure 8) exhibits typical resonance features. The triangle-like form of imaginary parts of the spectral function is more pronounced at high concentrations of inclusions than at lower p. This can be attributed to the larger relative amount of 'long' clusters at high concentrations, i.e., those related to the poles located at low s.

Obtained frequency dependences of intrinsic permeability for both the magnetic powders exhibit the magnetic absorption maximum at very low frequencies. Because of that, the observed magnetic spectra can be attributed to the domain wall motion rather than to ferromagnetic resonance. However, the magnetic spectra related to the domain walls are described adequately by the model discussed in the previous section. Indeed, in this case Snoek's law is also valid [24] and the frequency dependence of the permeability has the same form (14) as for the ferromagnetic resonance [29].

The results of the study are validated by the comparison of the values of the parameters given in table 1 with those obtained by independent estimation. Snoek's constant S of carbonyl iron obtained in this study as 50–60 GHz is in close agreement with the theoretical value of 40 GHz typical for pure iron. The average skinning parameter θ, that is 0.3 for carbonyl iron

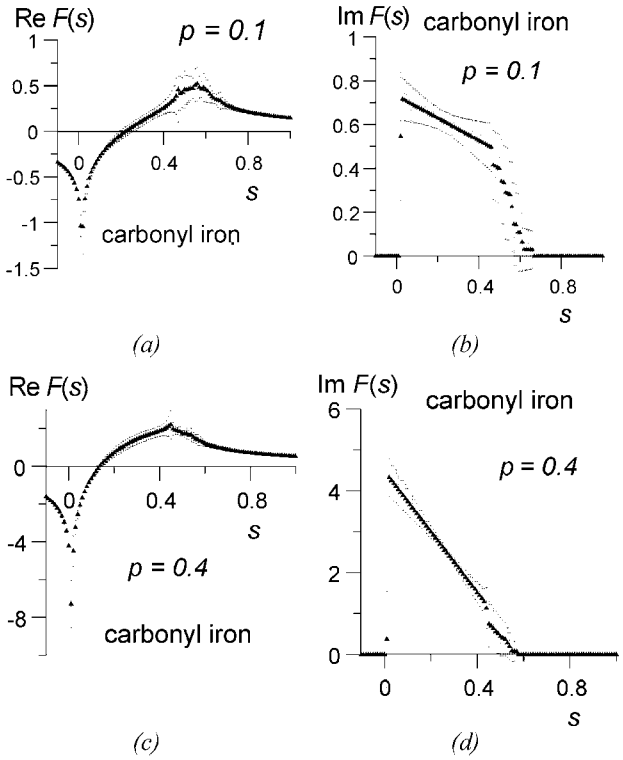

Figure 9. The average values (triangles) and the standard deviation of reconstructed spectral functions for the investigated composites filled with carbonyl iron powder at different concentrations p: (a) the real part and (b) the imaginary part of $F(s)$ for $p = 0.1$; (c) the real part and (d) the imaginary part of $F(s)$ for $p = 0.4$.

and 1.6 for the alloy, also correlates well with the theoretical values. The theoretical estimate for θ is $\theta = 0.27$ for carbonyl iron with the conductivity 2×10^6 S m^{-1} and the mean radius $a = 3$ μm and $\theta = 1.7$ for the alloy with the conductivity 7.7×10^5 S m^{-1} and $a = 30$ μm. This confirms the validity of the model used.

It is of interest to discuss the values of the damping factor α obtained in this study. As follows from table 1, the value of α for carbonyl iron is much larger than that of Fe–Cr–Al alloy. This can be attributed to the fact that carbonyl iron possesses an onion-like structure. In the treatment of the magnetic properties of an iron particle this structure can be allowed for by introducing the effective porosity of the particle [30]. As shown in [30], the porosity results in broadening the ferromagnetic resonance line, that can be approximately evaluated as

$$\Delta H \cong 1.5(4\pi M_s)\frac{p_0}{1+p_0}, \tag{17}$$

where p_0 is the volume concentration of pores. The carbonyl iron is known to contain approximately 1% of carbon interlayers [28]. Then, as $M_s = 1700$ G for pure iron, (17) yields $\Delta H = 320$ Oe. From this value, the relaxation time $\tau = (\gamma \Delta H/2)^{-1}$ is estimated as 3.6×10^{-10} s and the damping factor $\alpha = 1/(2\pi f_0 \tau)$ as $\alpha \cong 3$ on the assumption that the average resonance frequency is $f_0 = 0.15$ GHz. This value agrees with the results of this study. The Fe–Cr–Al alloy is manufactured by melting. Hence its particles should be more homogeneous and the value of damping factor should be less, as follows from the data obtained.

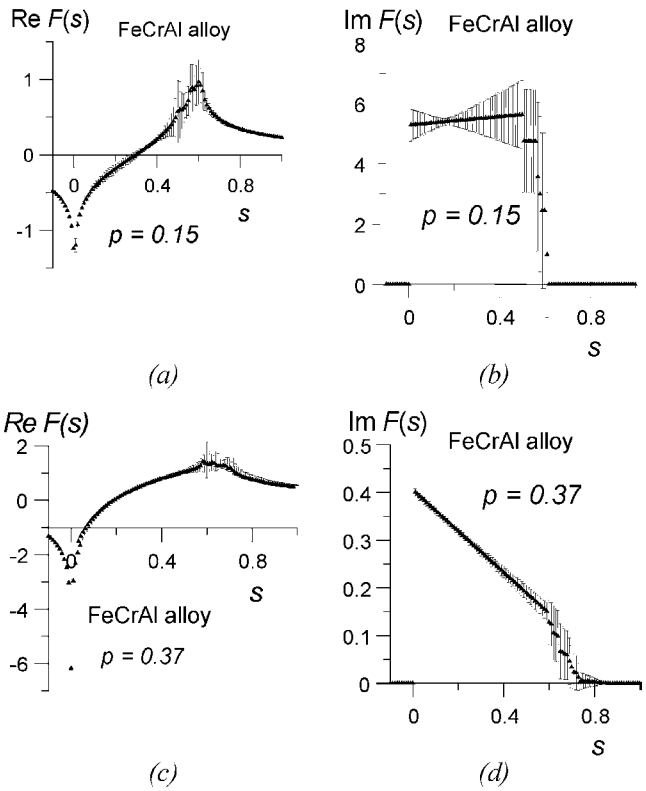

Figure 10. The average values (triangles) and the standard deviations of reconstructed spectral functions for the investigated composites filled with FeCrAl (13.6 at.% Cr–6 at.% Al–80.4 at.% Fe) alloy powder at different concentrations p: (a) the real part and (b) the imaginary part of $F(s)$ for $p = 0.15$; (c) the real part and (d) the imaginary part of $F(s)$ for $p = 0.37$.

5. Conclusion

The obtained results reveal that the measured frequency dependence of microwave permeability of composites filled with magnetic powder provides enough data to estimate both intrinsic permeability of the inclusions and the spectral function of the composite. In this paper, composites filled with carbonyl iron and Fe–Cr–Al alloy powders are under study. Data on the spectral function of actual composites are obtained. The results are in agreement with available tabulated data.

The uncertainty in the obtained data is rather high. The main reason is that the problem is ill conditioned from the mathematical standpoint. To reduce the uncertainty, certain simplifications of the model are introduced, which allow the model to be more definite. On the other hand, these simplifications also enhance the uncertainty, and the total accuracy of the obtained data is as low as about 30%.

To improve the accuracy and obtain further validation of the results, more data are needed in the data processing. A promising approach is to process the measured data on the permittivity and permeability together with the data on other transport properties of the sample such as heat conductivity, etc. As all the transport properties are governed by the same spectral function, this would increase the number of data involved in the computation and thus diminish the uncertainty.

More validation of the results could be obtained by adding the data provided by direct techniques for examining the structure of composites, e.g., by microscopic determination of the particle distribution. Technological means for producing the samples with the prescribed microstructure can also be useful.

Certain development of the approach is possible with more utilization of the data on microwave properties of composites. For example, wideband data on the frequency dependence of complex permittivity could be added. However, in the powder-filled composites under study the dispersive area is located in the IR region. Introducing these data would require the application of IR measuring techniques and the account of the frequency dependence of conductivity of the inclusions. Both these factors increase the uncertainty. The dielectric dispersion of the powder-filled composites manifests itself at microwaves through the frequency dependent dielectric loss, with the dielectric loss tangent being very small. The analysis of the low frequency dielectric dispersion allows the derivative of $F(s)$ at $s = 0$ to be determined.

Finally, the measurement of the effective permeability under magnetic bias seems to be a very promising technique to improve the approach described in this paper. This technique is in some sense complementary to the simultaneous processing of the data related to different volume fraction of inclusions. Indeed, the biasing field affects the intrinsic permeability with the spectral function remaining unchanged, while the difference in volume fraction affects the spectral function and does not influence the intrinsic permeability. The study of the intrinsic permeability of magnetic powders under biasing field is a powerful tool for understanding the structure and properties of these powders.

Acknowledgments

The authors are grateful to Professor I T Iakubov and Professor K M Hock for valuable remarks. The study was partially supported by RFBR, agreements no 01-02-17962 and 00-15-96570.

References

[1] Neelakanta P S 1995 *Handbook of Electromagnetic Material* (Boca Raton, FL: Chemical Rubber Company Press)
[2] Bergman D J 1976 *Phys. Rev.* B **14** 1531
[3] Milton G W 1980 *Appl. Phys. Lett.* **37** 300
[4] Landauer R 1978 *Electrical Transport and Optical Properties of Inhomogeneous Media (AIP Conf. Proc. No 40 Part 2)* ed J C Garland *et al* (New York: American Institute of Physics) p 2
[5] Maxwell Garnett J C 1904 *Phil. Trans. R. Soc.* A **203** 385
[6] Bruggeman D A G 1935 *Ann. Phys., NY* **24** 636
[7] Sheng P and Calleragi A G 1984 *Appl. Phys. Lett.* **44** 738
[8] McLachlan D S, Priou A, Chenerie I, Isaak E and Henry F 1992 *J. Electromagn. Waves Appl.* **6** 1099
[9] Niklasson G A and Granquist C G 1984 *J. Appl. Phys.* **55** 3382
[10] Miyasaka K, Watanabe K, Jojima E, Aida H, Sumita M and Ishikawa K 1982 *J. Mater. Sci.* **17** 1610
[11] Egu W G and Apsnes D E 1982 *Phys. Rev.* B **26** 5313
[12] Lagarkov A N, Matytsin S M, Rozanov K N and Sarychev A K 1998 *J. Appl. Phys.* **84** 3806
[13] Pitman K C, Lindley M W, Simkin D and Cooper J F 1991 *IEE Proc.* F **138** 223
[14] Milton G W 1981 *Appl. Phys.* **26** 125
[15] Bergman D J 1979 *Phys. Rev.* B **19** 2359
[16] Bergman D J and Dunn K-J 1992 *Phys. Rev.* B **45-I** 13 262
[17] Bergman D J 1986 *Homogenization and Effective Moduli of Materials and Media* ed J L Ericsen *et al* (New York: Springer) p 27
[18] Bergman D J and Stroud D 1992 *Solid. State Phys.* **46** 147
[19] Bergman D J 1978 *Phys. Rep.* **43** 377
[20] Day A R, Grant A R, Sievers A J and Thorpe M F 2000 *Phys. Rev. Lett.* **84** 1978

[21] Hornfeck M, Theiss W and Clasen R 1992 *J. Non-Cryst. Solids* **145** 154
[22] Odelevski V I 1951 *Sov. Phys.–JETP* **21** 667
[23] Dykhne A M 1970 *Sov. Phys.–JETP* **59** 110
[24] Soohoo R F 1985 *Microwave Magnetics* (New York: Harper and Row) p 120
[25] Gurevich A G and Melkov G A 1994 *Magnetic Ocsillations and Waves* (Moscow: Nauka)
[26] Lewin L 1951 *Advanced Theory of Waveguides* (London: Illife)
[27] Taylor J R 1962 *An Introduction to Error Analysis* (Mill Valley: University Science Books)
[28] Volkov V L and Syrkin V G 1969 *Carbonyl Iron* (Moscow: Metallurgiya)
[29] Bouchaud J P and Zerah P G 1990 *J. Appl. Phys.* **67** 5512
[30] Schloemann E 1957 *Proc. 2nd Conf. on Magnetism and Magnetic Materials (Boston, MA, 1956)* p T-91